Supporting Information

Excited-State Charge Transfer and Extended Charge Separation within Covalently-Tethered Type-II CdSe/CdTe Quantum Dot Heterostructures: Colloidal and Multilayered Systems

Caitlin R. McGranahan, Guy E. Wolfe II, Alejandro Falca, and David F. Watson*

*Corresponding Author: dwatson3@buffalo.edu

Department of Chemistry, University at Buffalo, The State University of New York, Buffalo, New York 14260-3000, United States

Table of Contents

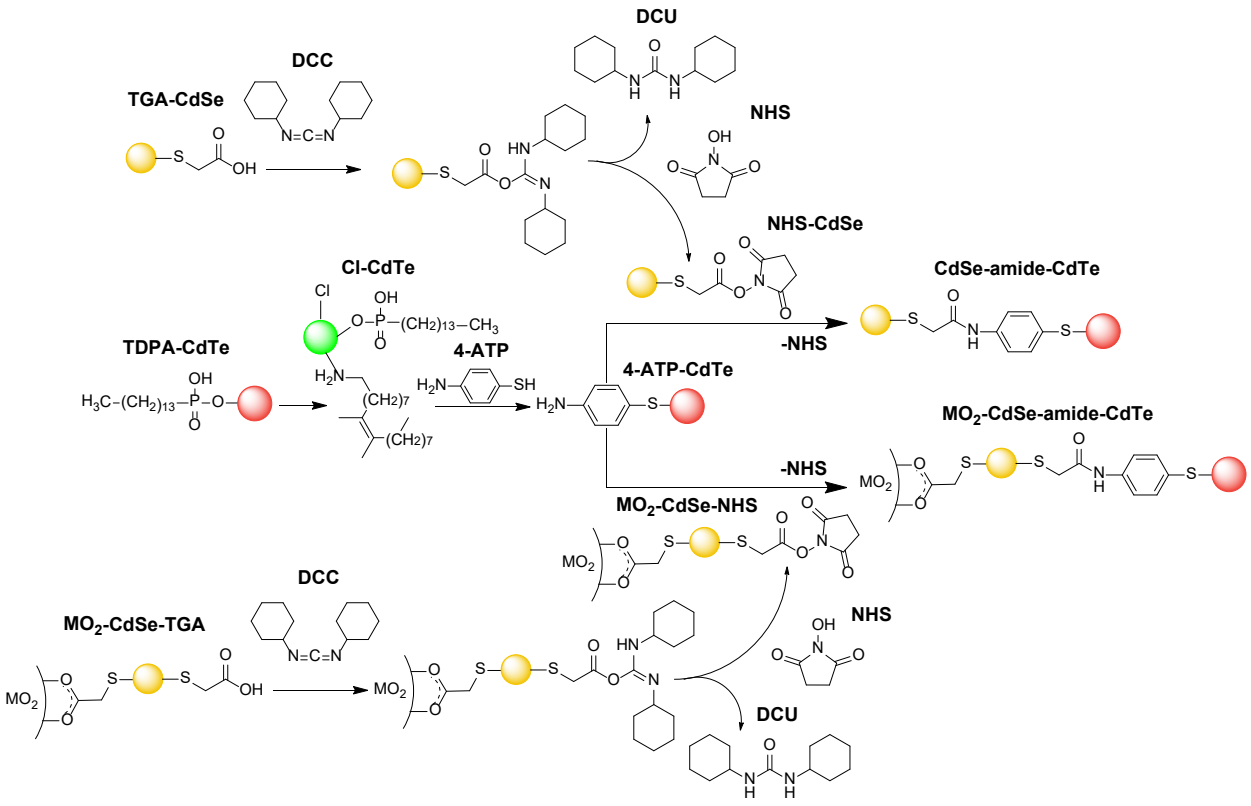

Scheme S1. Targeted carbodiimide-mediated coupling mechanism by which CdSe and CdTe QDs are covalently tethered both in dispersion and adsorbed to thin films. QDs are not drawn to scale, and surface chemistry is represented by individual adsorbates.

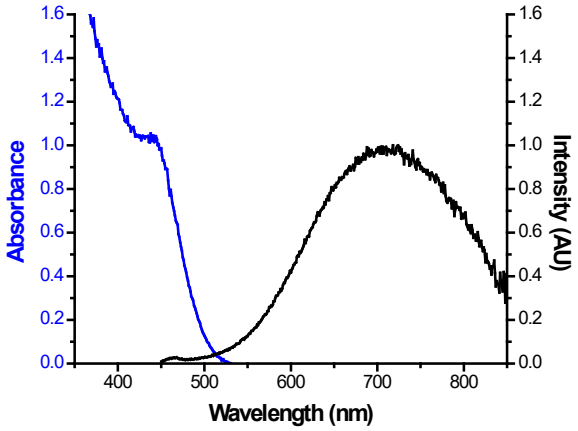

Figure S1. Absorbance spectrum (blue) and emission spectrum (black) of an aqueous dispersion of TGA-CdSe QDs.

Table S1. Wavenumbers and assignments of prominent bands in the ATR-FTIR spectra within Figure 1.

Sample	Peak Number	Wavenumber (cm^{-1})	Assignment	References
TGA-CdSe	1	1227	C-O stretch (ν(CO))	[1, 2]
	2	1384	CO_2^- symmetric stretch ($\nu_s(CO_2^-)$)	[1, 2]
	3	1568	CO_2^- asymmetric stretch ($\nu_a(CO_2^-)$)	[1, 2]
	4	3385	O-H stretch (ν(OH))	[3]
NHS-CdSe	1	1223-1245	C-O stretch (ν(CO)), CNC asymmetric stretch (ν_a(CNC))	[1, 2, 4]
	2	1375	CO_2^- symmetric stretch ($\nu_s(CO_2^-)$)	[1, 2]
	3	1546	CO_2^- asymmetric stretch ($\nu_a(CO_2^-)$)	[1]
	4	1626	NHS stretch (ν(CON))	[5]
	5	1710	Imidyl asymmetric stretch (ν_a(O=C-N-C=O))	[5]
	6	1740	Imidyl symmetric stretch (ν_s(O=C-N-C=O))	[5]
	7	2931	CH_2 asymmetric stretch ($\nu_s(CH_2)$)	[2]
	8	3280	O-H stretch (ν(OH))	[3]

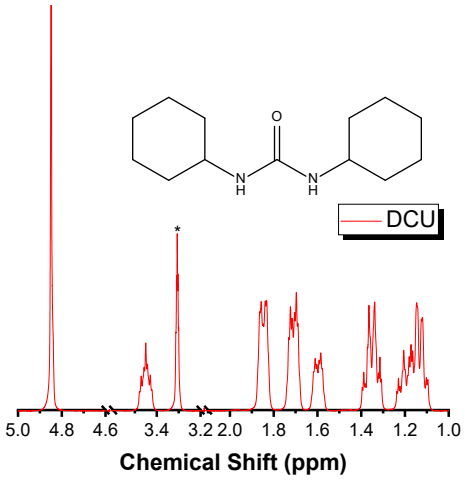

Figure S2. ^{1}H NMR spectrum (500 MHz, methanol-d_4) of DCU as an isolated stable byproduct of the carbodiimide-mediated coupling reaction between NHS and TGA-CdSe QDs. The asterisk indicates the solvent peak.

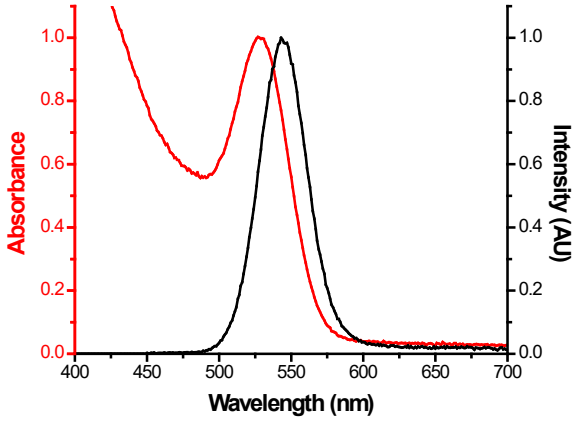

Figure S3. Absorbance spectrum (red) and emission spectrum (black) of toluene-dispersed TDPA-CdTe QDs.

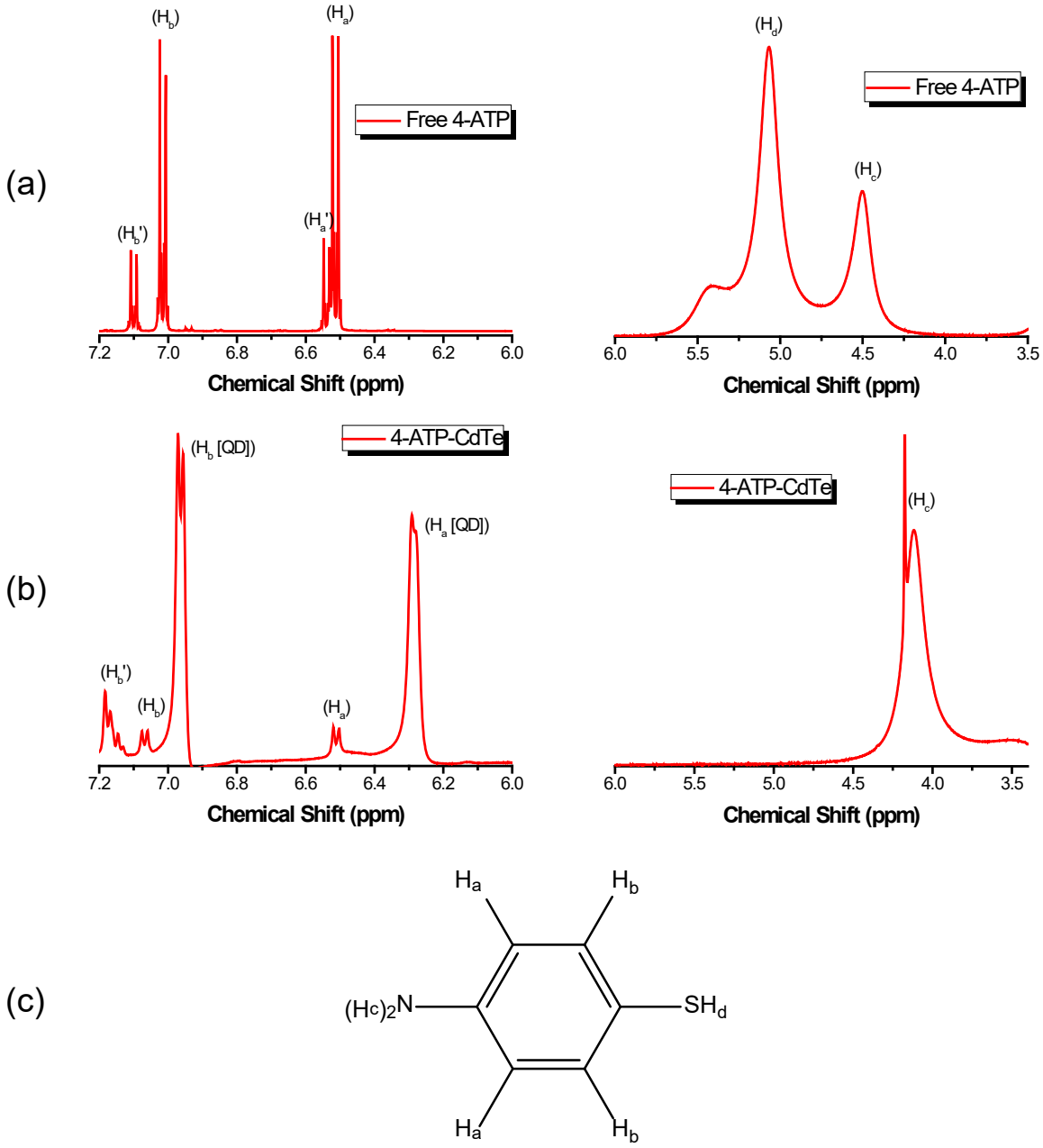

Figure S4. Two regions of ^{1}H NMR spectrum (500 MHz, DMSO-d_6) of free 4-ATP (a) and 4-ATP-CdTe QDs (b) with resonances assigned according to structure (c).

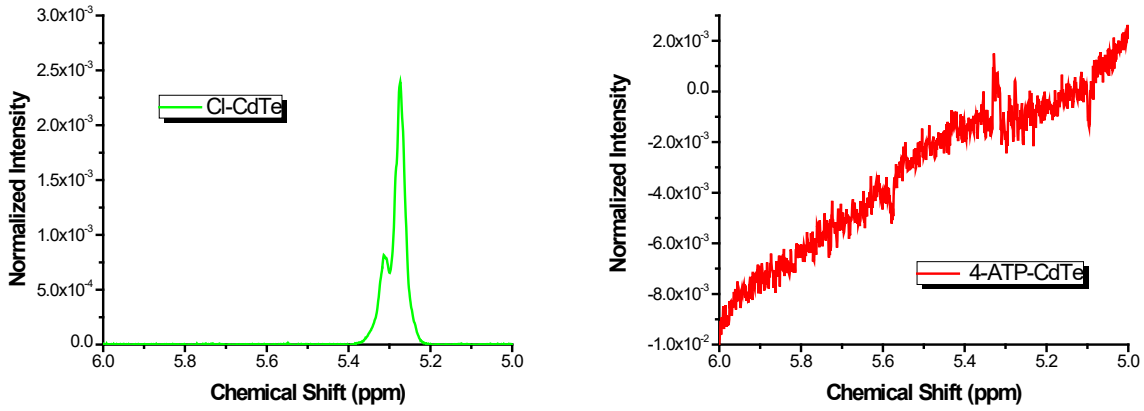

Figure S5. ^{1}H NMR spectrum of Cl-CdTe QDs (500 MHz, $CDCl_3$) and 4-ATP-CdTe QDs (500 MHz, DMSO-d_6). Spectra are normalized to a residual solvent resonance.

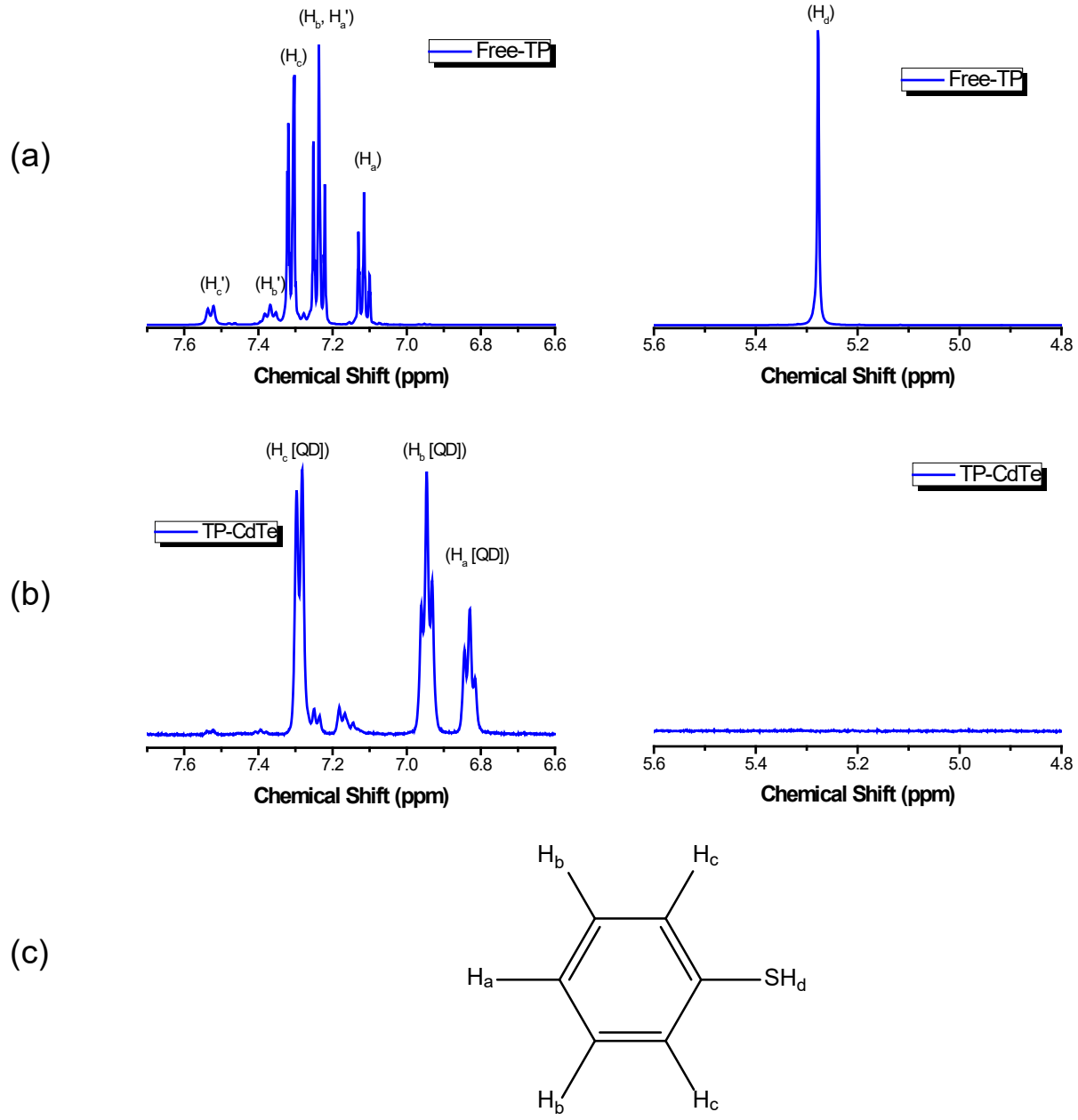

Figure S6. Two regions of ^{1}H NMR spectrum (500 MHz, DMSO-d_6) of free TP (a) and TP-CdTe (b) with resonances assigned according to structure (c).

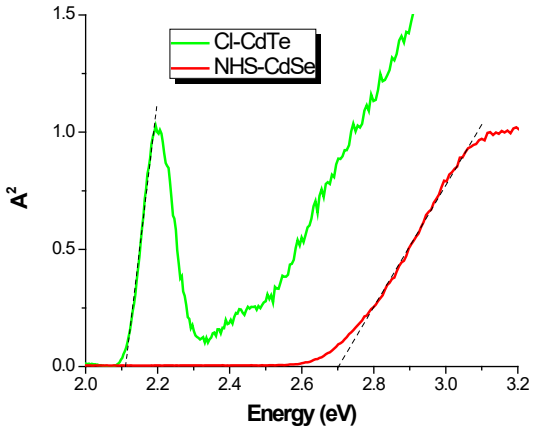

Figure S7. Square of absorbance (A^2) as a function of energy for Cl-CdTe QDs and NHS-CdSe QDs dispersed in DMSO. Superimposed (black dashed lines) are linear fits of the first excitonic absorption bands.

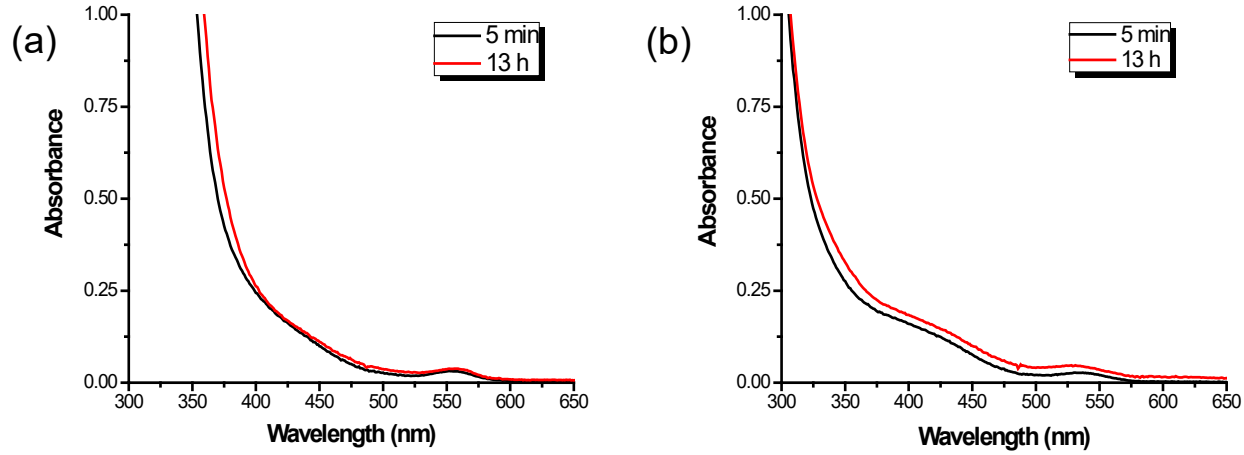

Figure S8. Absorbance spectra of CdSe-/-CdTe (a) and CdSe-amide-CdTe (b) dispersions in DMSO over time.

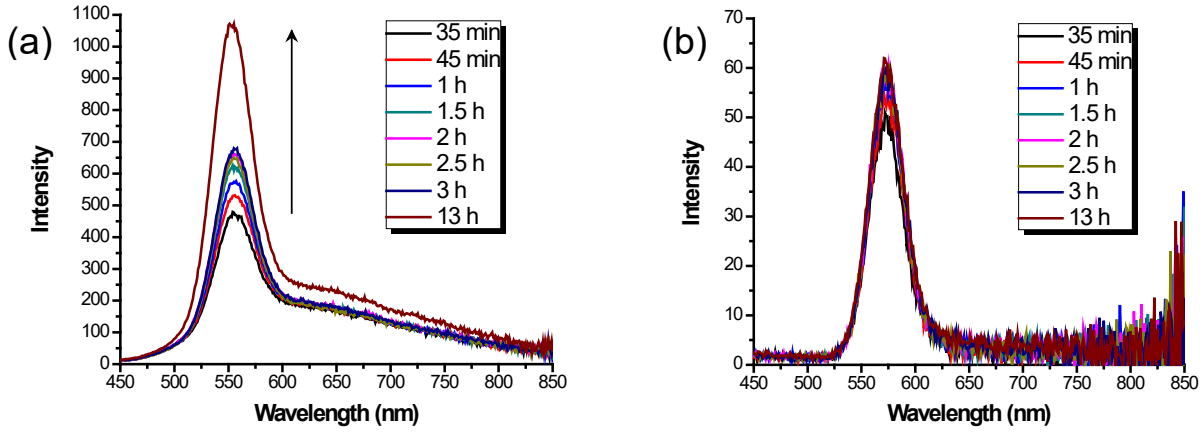

Figure S9. Steady-state emission spectra of CdSe-/-CdTe (a) and CdSe-amide-CdTe (b) dispersions in DMSO over time. Spectra on different y-axis scales due to the quenching of emission for CdSe-amide-CdTe dispersions (b).

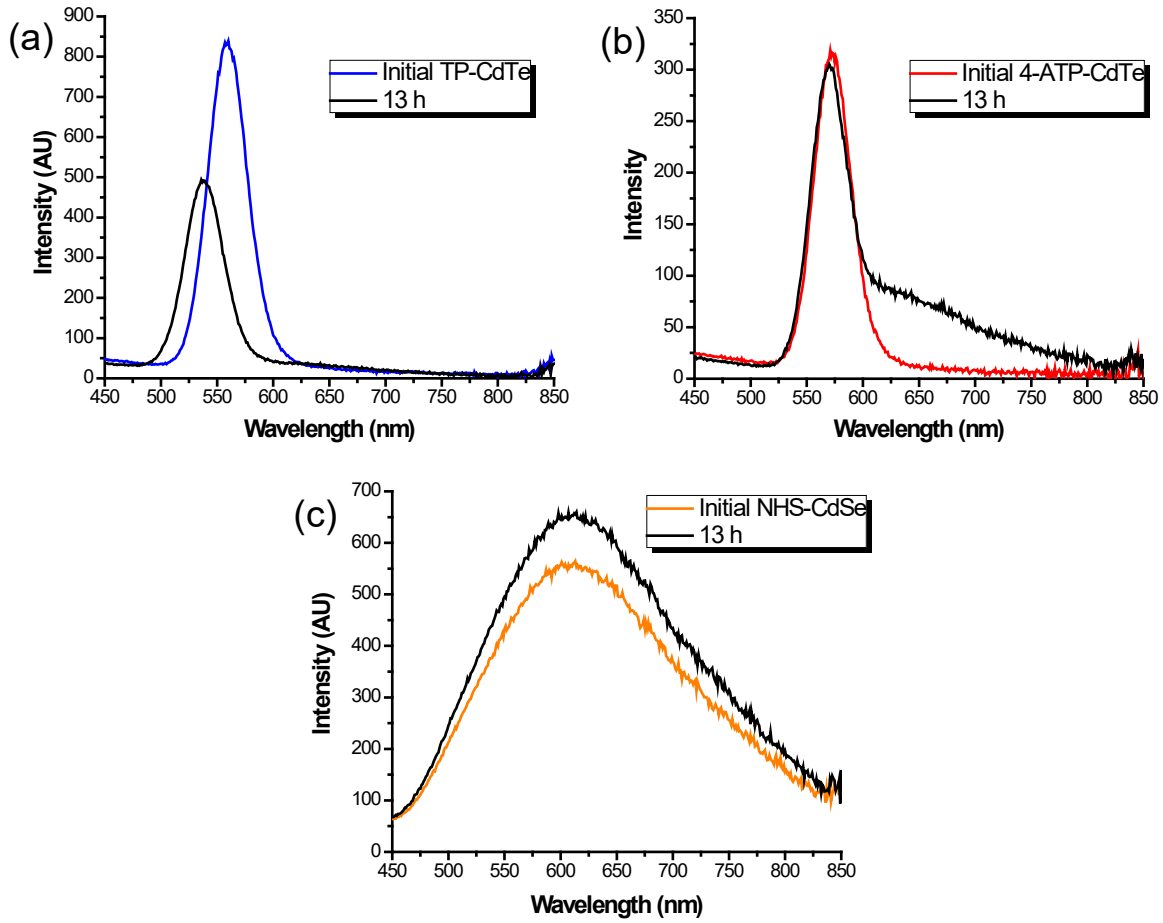

Figure S10. Steady-state emission spectra of isolated TP-CdTe QDs (a), 4-ATP-CdTe QDs (b), and NHS-CdSe QDs (c) dispersions in DMSO over time.

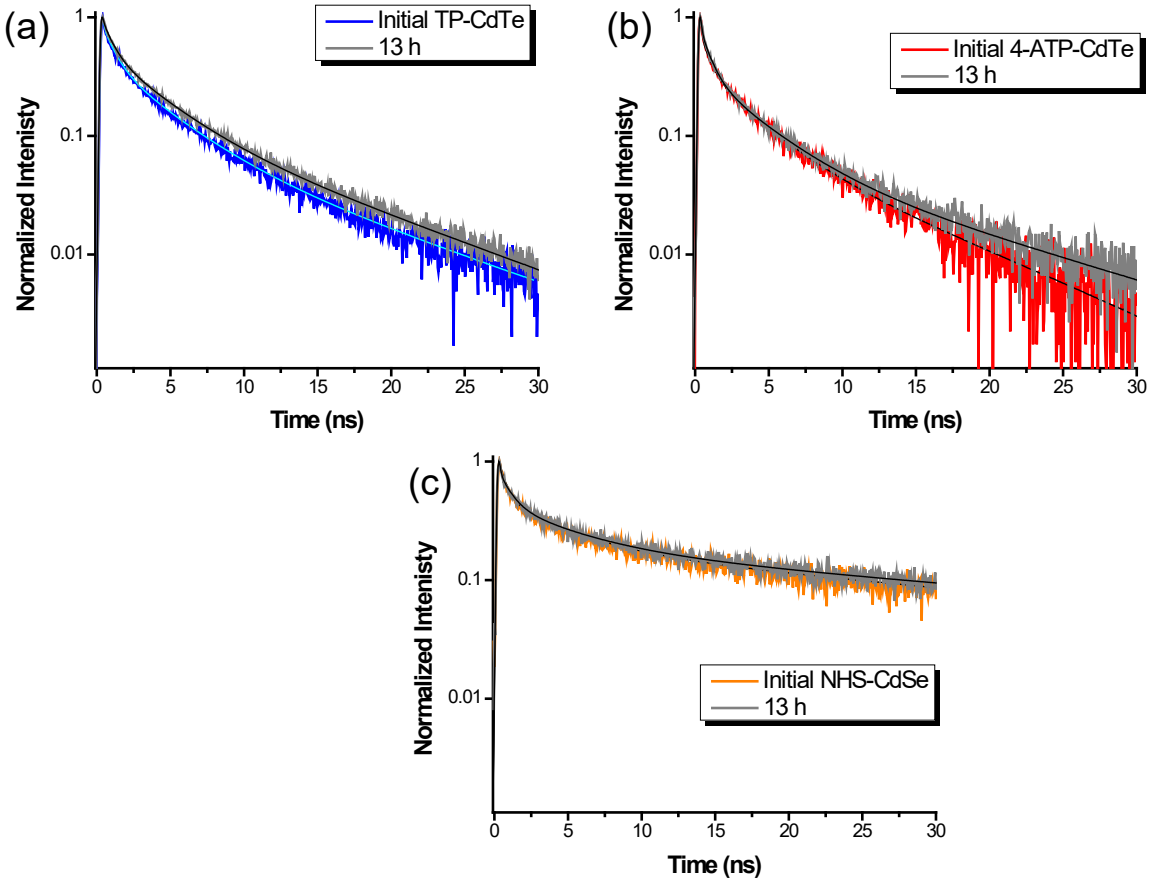

Figure S11. Time-resolved emission decay traces of isolated TP-CdTe QDs at 534 nm (a), 4-ATP-CdTe QDs at 534 nm (b), and NHS-CdSe QDs at 664 nm (c) dispersions following pulsed excitation at 445 nm. Superimposed on the decay traces are fits to triexponential decay kinetics.

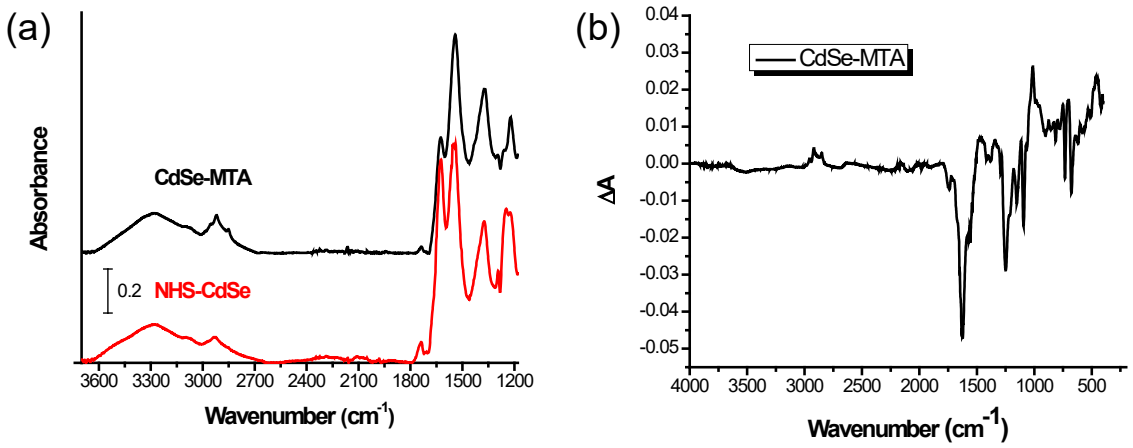

Figure S12. ATR-FTIR spectra of NHS-CdSe (red) and CdSe-MTA QDs (black) (a) and the difference spectrum between the spectral features of CdSe-MTA and NHS-CdSe (b). Spectra in (a) are offset for clarity.

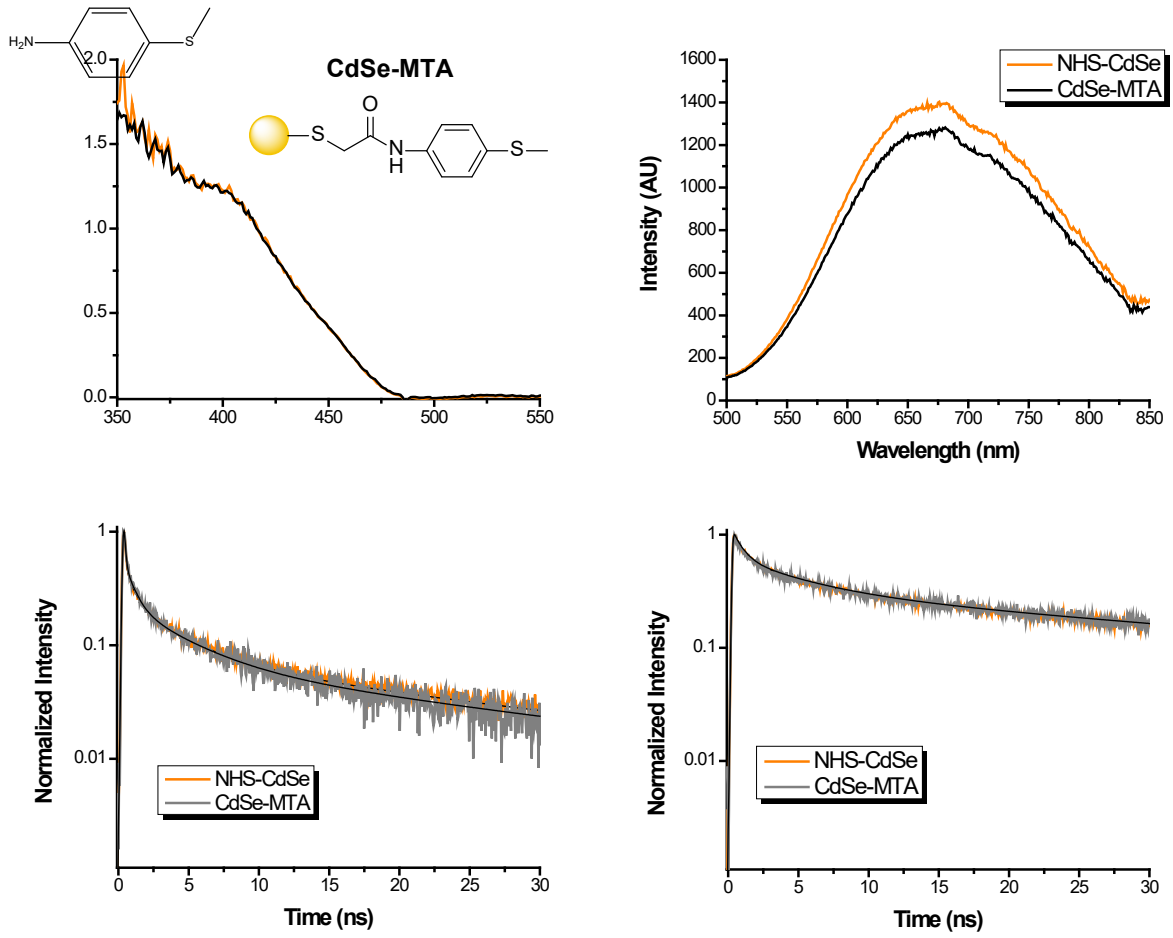

Figure S13. Absorbance spectra (a), steady-state emission spectra (b), and time-resolved emission decay traces at 546 nm (c) and 678 nm (d) of NHS-CdSe (orange) and CdSe-MTA (black). Superimposed on the decay traces are fits to triexponential decay kinetics.

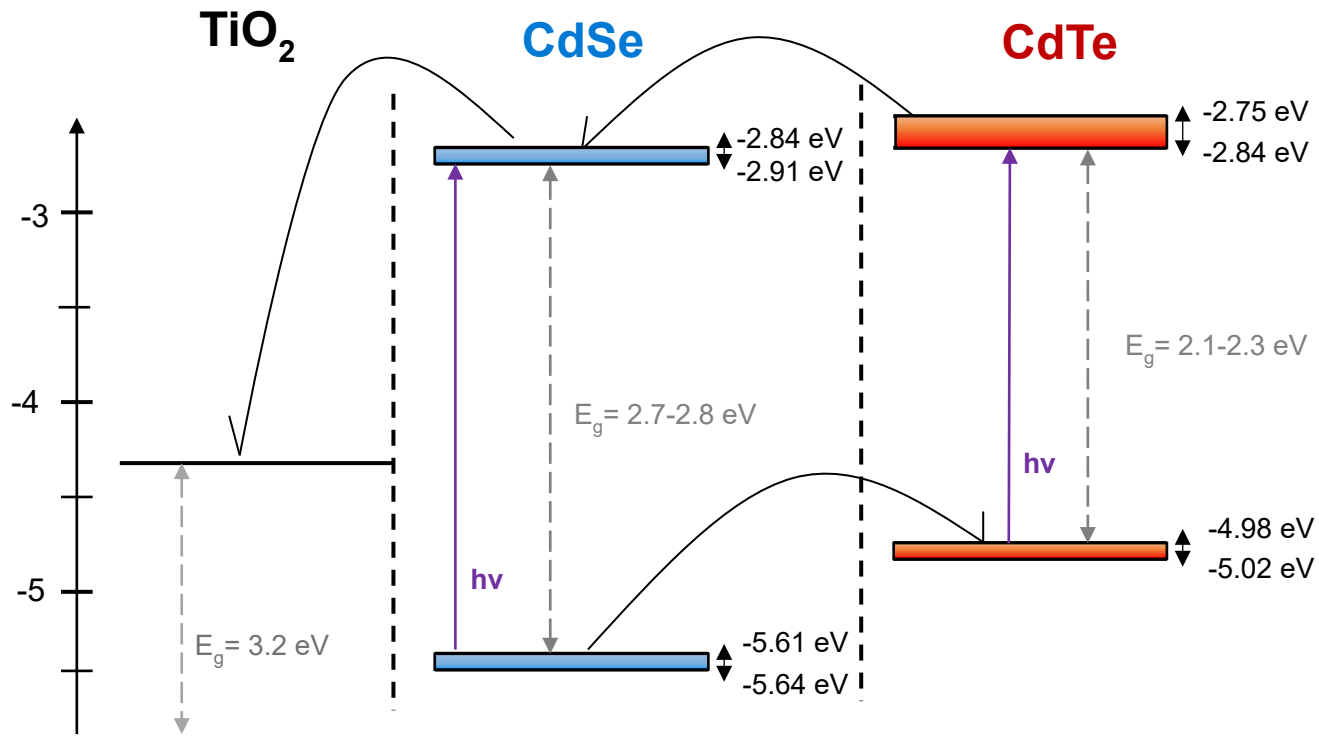

Figure S14. Estimated energy-level diagram for TiO_2-CdSe-amide-CdTe ternary heterostructures with ranges of valence and conduction band-edge potentials from different synthetic batches.

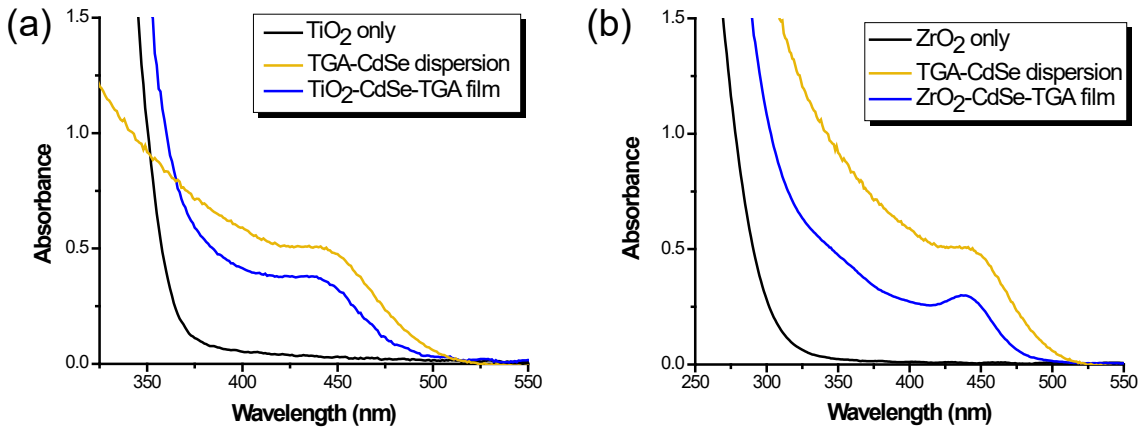

Figure S15. Absorbance spectra of aqueous dispersions of TGA-CdSe QDs, unfunctionalized TiO_2 films, and TiO_2-CdSe-TGA films (a) and aqueous dispersions of TGA-CdSe QDs, unfunctionalized ZrO_2 films, and ZrO_2-CdSe-TGA films (b).

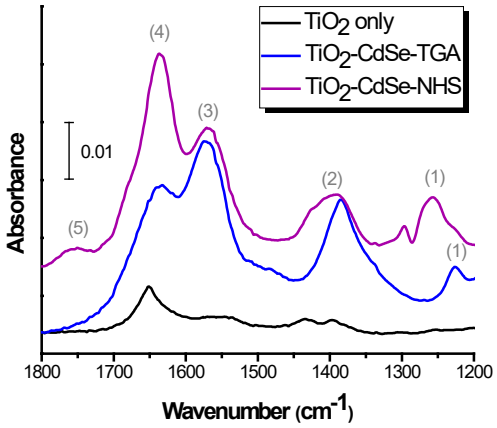

Figure S16. ATR-FTIR spectrum of unfunctionalized TiO_2 films (black), TiO_2-CdSe-TGA films (blue), and TiO_2-CdSe-NHS films (grey). Peak assignments refer to Table S2 and the spectra are offset for clarity.

Table S2. Wavenumbers and assignments of prominent bands on the ATR-FTIR spectra within Figure S16.

Sample	Peak Number	Wavenumber (cm^{-1})	Assignment	References
TiO_2-CdSe-TGA	1	1227	C-O stretch (ν(CO))	[1, 2]
	2	1386	CO_2^- symmetric stretch ($\nu_s(CO_2^-)$)	[1, 2]
	3	1571	CO_2^- asymmetric stretch ($\nu_a(CO_2^-)$)	[1, 2]
	4	1636	TiO_2-OH bending mode ($\delta(TiO_2\text{-}OH)$)	[6]
TiO_2-CdSe-NHS	2	1392-1427	CO_2^- symmetric stretch ($\nu_s(CO_2^-)$),	[1, 2, 4]
	4	1639	TiO_2-OH bending mode ($\delta(TiO_2\text{-}OH)$), NHS stretch (ν(CON))	[6, 7]
	5	1712-1775	Imidyl symmetric and asymmetric stretches ($\nu_{s,a}$(O=C-N-C=O))	[8]

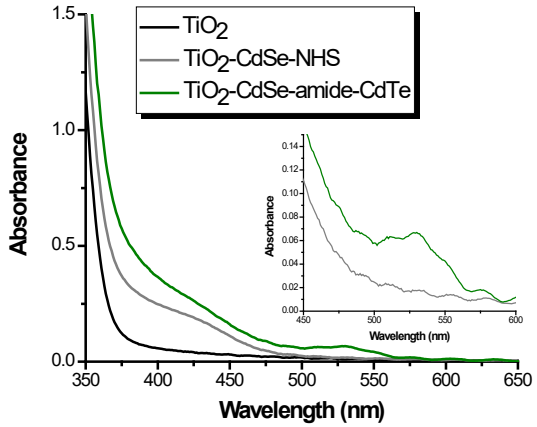

Figure S17. Absorbance spectra of TiO_2-CdSe-NHS and TiO_2-CdSe-amide-CdTe films.

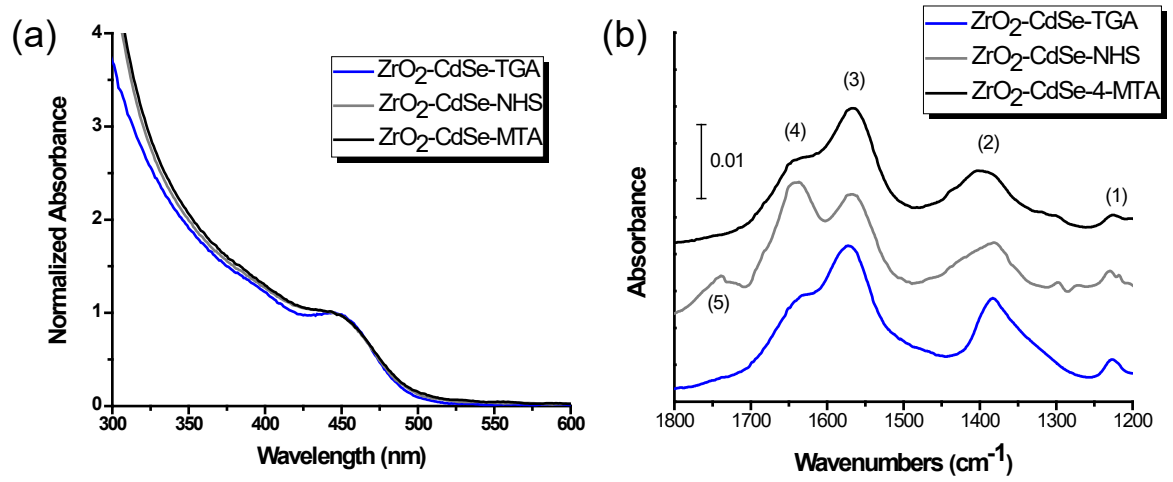

Figure S18. UV-Vis absorbance spectra (a) and ATR-FTIR spectra (b) of ZrO_2-CdSe-TGA (blue), ZrO_2-CdSe-NHS (grey), and ZrO_2-CdSe-MTA (black) films. Spectra are offset for clarity.

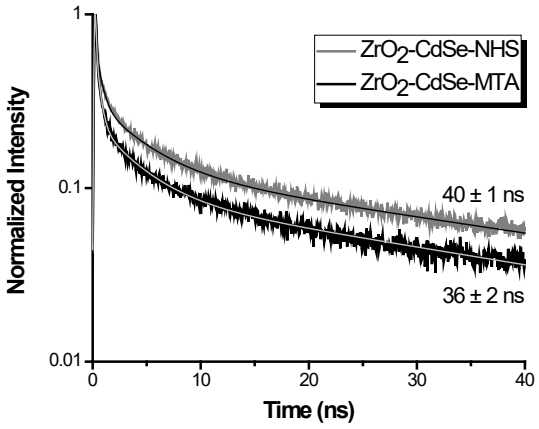

Figure S19. Time-resolved emission decay traces of ZrO_2-CdSe-NHS (grey) and ZrO_2-CdSe-MTA (black) films. Superimposed on the decay traces are fits to triexponential decay kinetics.

Appendix S1.1. Materials.

Reagents were obtained from the following commercial sources: (1) Alfa Aesar [1-octadecene (ODE) (tech. 90%), 4-aminothiophenol (4-ATP) (97%), cadmium chloride 2.5-hydrate (79.5-81.0%), cadmium oxide (Puratronic, 99.998%), N',N'-dicyclohexylcarbodiimide (DCC) (99%), thiophenol (TP) (99+%), tri-*n*-octylphosphine (TOP) (90%)]; (2) Fisher Scientific [nitric acid (65% w/w), sodium sulfite anhydrous (98%)]; (3) Honeywell [cadmium chloride anhydrous (99.0+%)]; (4) Macron Fine Chemicals [sodium hydroxide, pellet]; (5) Sigma-Aldrich [4-(methylthio)aniline (4-MTA) (98%), methanol anhydrous (99.8%), *N*-hydroxysuccinimide (NHS) (98%), oleylamine (OLA) (98+%), polyethyleneglycol bisphenol A epichlorohydrin copolymer (PEG), selenium powder (>99.5%), tellurium powder (200 mesh, 99.8%), tetradecylphosphonic acid (TDPA) (99+%), thioglycolic acid (TGA) (98+%), titanium(IV) isopropoxide (97%), trioctylphosphine oxide (TOPO) (99%), zirconium(IV) propoxide (70 wt. % in 1-propanol). Acetone, chloroform ($CHCl_3$), dimethylformamide (DMF), dimethyl sulfoxide (DMSO), deuterated dimethyl sulfoxide (DMSO-d_6), hexanes, methanol (MeOH), tetrahydrofuran (THF), and toluene were obtained from various commercial sources. Reagents and solvents were used as received.

Appendix S1.2. Detailed descriptions of reported synthetic methods.

Synthesis of TGA-capped CdSe QDs for Dispersions.

A solution of sodium selenosulfate (Na_2SeSO_3) was prepared by combining Se (175.3 mg, 2.22 mmol) and Na_2SO_3 (801.0 mg, 6.35 mmol) in deionized (DI) water (42 mL). The solution was allowed to reflux for 16-24 h to dissolve the Se. A solution of $CdSO_4 \cdot 8H_2O$ (194 mg, 0.252 mmol) and TGA (0.200 mL, 2.87 mmol) in DI H_2O (18 mL) was prepared. The pH was adjusted to 12.4 with NaOH pellets. The cadmium-containing solution was then heated to 80 °C, and 7.5 mL of the Na_2SeSO_3 solution was added quickly. The reaction mixture was maintained at 80°C for 1 h. The resulting TGA-CdSe QDs were flocculated with MeOH and collected by centrifugation. The supernatant was discarded, and the QDs were washed with excess MeOH two additional times to remove unreacted precursors.

Synthesis of TGA-CdSe QDs for Thin Films.

A Na_2SeSO_3 solution was prepared by combining selenium powder (0.530 g, 6.71 mmol, 0.084 M) and sodium sulfite (2.33 g, 0.018 mol, 0.231 M) in DI water (80 mL). This mixture was allowed to reflux for several hours until it became clear. A solution of $CdCl_2 \cdot 2.5\ H_2O$ (3.00 g, 0.013 mol, 0.155 M) and TGA (5.00 mL, 0.072 mol, 0.847 M) in DI H_2O (80.0 mL) was prepared. The pH of this solution was adjusted to 6.5 using NaOH pellets. The selenide- and cadmium-containing solutions were combined and heated under reflux (30 min). The resulting TGA-CdSe QDs were flocculated with excess acetone and collected by centrifugation.

Synthesis of Metal Oxide Pastes.

Either zirconium(IV) propoxide (50.0 mL, 52.2 g, 0.159 mol) or titanium(IV) isopropoxide (50.0 mL, 48.0 g, 0.169 mol) was added dropwise to an aqueous solution (300 mL) of nitric acid

(0.167 M) over the course of several minutes and heated at 80 °C until the remaining volume was 90 mL. The resulting mixture (9.0 mL) was placed in a Parr bomb overnight at 200 °C. PEG was added (0.5 g, ~0.03 mmol) to produce either a ZrO_2 or TiO_2 paste with a concentration of 60 g/L with constant stirring.

Preparation of NHS-Ester-Capped CdSe QDs for Dispersions.

Dried TGA-CdSe QDs (10.0 mg) were dispersed in DI H_2O (20 mL). The pH of the resulting dispersions was adjusted from approximately 10 to 6.9 with dilute HNO_3 to prevent hydrolysis of the desired NHS-ester. DCC (100 mg, 0.48 mmol) and NHS (100 mg, 0.87 mmol) were added simultaneously to a mixture of dispersed TGA-CdSe QDs (5 mL) and DMF (20 mL). The resulting mixture was stirred overnight at room temperature in the dark. DCU precipitated and was removed by centrifugation. The resulting dispersion of NHS-ester-capped CdSe QDs, hereafter referred to as NHS-CdSe QDs, was flocculated with excess THF. The QDs were washed three times with excess THF, to remove free NHS, DCC, and DCU, and then dispersed in DMSO.

Preparation of NHS-Ester-Capped CdSe QDs for Thin Films.

NHS (0.500 g, 4.34 mmol, 0.043 M) and DCC (0.500 g, 2.42 mmol, 0.024 M) were dissolved in DMF (100. mL). ZrO_2-CdSe-TGA or TiO_2-CdSe-TGA films were submerged in the resulting solution and allowed to equilibrate overnight at room temperature. DCU precipitated in small amounts as confirmed by ^{1}H NMR. The modified NHS-ester-capped CdSe QDs on the metal oxide substrates, hereafter referred to as TiO_2- or ZrO_2-CdSe-NHS, were removed from the immersion solution, dipped in neat DMF solvent, and dried using THF.

Synthesis of TDPA-capped CdTe QDs.

A solution of CdO (0.255 g, 1.99 mmol, 0.050 M) and TDPA (1.20 g, 4.31 mmol, 0.108 M) in ODE (40.0 mL, 0.125 mol) was prepared. This solution was deaerated under argon (30 min) and then heated to 300 °C with constant stirring. In a separate flask, a solution of Te (0.255 g, 2.00 mmol, 0.200 M) in TOP (10.0 mL, 22.0 mmol) was prepared under an inert atmosphere and sealed with a rubber septum. The Te-containing solution was diluted with ODE (10.0 mL, 0.031 mol), heated to 200 °C, and then quickly injected into the Cd-containing solution. Once the desired particle size was achieved, as evidenced by the first-excitonic absorption maximum of CdTe, the reaction mixture was quenched by removal of heat. The resulting TDPA-CdTe QDs were extracted using MeOH and hexanes in a 1:1 ratio (v/v). The QDs were centrifuged to remove impurities. The hexane-dispersed TDPA-CdTe QDs were then flocculated with excess acetone, collected by centrifugation, and stored in the dark.

Chloride Treatment of TDPA-CdTe QDs.

A stock solution of $CdCl_2$ (0.33 M) was prepared by combining anhydrous $CdCl_2$ (0.300 g, 1.64 mmol, 0.327 M) and TDPA (0.033 g, 0.119 mmol, 0.0237 M) in OLA (5.00 mL, 0.0152 mol) and deaerating with Ar (15 min). TDPA-CdTe QDs were dispersed in chloroform and gently refluxed. The absorbance at the first excitonic absorption maximum, and volume of the QD dispersion, were used to calculate the amount of $CdCl_2$ stock solution needed to provide 96 Cl^- ions/nm^2 of CdTe surface area. The desired volume was then injected (~80 °C). Following the addition of the $CdCl_2$ solution, the reaction mixture was refluxed for 15 min. The resulting chloride-treated CdTe QDs, hereafter referred to as Cl-CdTe QDs, were flocculated with excess acetone, collected by centrifugation, and dispersed in toluene.

Ligand Exchange to Yield 4-ATP-capped CdTe QDs and TP-capped CdTe QDs.

To displace TDPA with 4-ATP, Cl-CdTe QDs (~1.19 x 10-5 mmol, ~1.98 x 10-3 mM) dispersed in toluene were added to a solution of 4-ATP (0.310 g, 2.48 mmol, 0.495 M) in toluene (5.0 mL) and reacted for 1 h to yield 4-ATP-capped CdTe QDs, hereafter referred to as 4-ATP-CdTe QDs. To displace TDPA with TP, TP (600 μL, 2.5 mmol, 0.50 mM) was added directly to dispersed Cl-CdTe QDs. The resulting mixture was and allowed to react for 24 h to yield TP-capped CdTe QDs, hereafter referred to as TP-CdTe QDs. The reaction mixtures were stirred in the dark, under an inert atmosphere, and collected by centrifugation. QDs were washed with excess MeOH to remove unbound ligands and then collected via centrifugation. This procedure was repeated twice, and then the CdTe QDs were dispersed in DMSO and stored in the dark.

Appendix 1.3. Spectroscopic characterization methods.

Steady-State Spectroscopy.

UV/vis absorption spectra were obtained using an Agilent 8453 diode array spectrophotometer, and diffuse reflectance spectra were obtained using a Labsphere RSA-HP-53 accessory. Photoluminescence spectra were obtained using a Varian Cary Eclipse fluorimeter with excitation ranging from 350-400 nm and emission from 450-850 nm. For time-dependent steady-state emission measurements, emission spectra of dispersions of QDs were compared to spectra of a solution of rhodamine 101 in EtOH to account for fluctuations of lamp intensity. ATR-FTIR spectra were collected using a Perkin-Elmer Spectrum Two spectrometer equipped with an ATR diamond accessory, with a wavenumber range of 4000-500 cm^{-1}. All ^{1}H NMR measurements were obtained using an Inova 500 MHz spectrometer. Each sample was scanned 1024 times, with an acquisition time of 2.05 s, and a relaxation time of 1.1 s.

Time-Resolved Emission.

Time-resolved emission measurements were obtained using a Becker and Hickl Tau-130 time-correlated single photon counting (TCSPC) instrument with a 16-channel photomultiplier tube. A pulsed diode laser (BDL-440 SMC) excited all samples at 445 nm (1 MHz, 40-90 ps, 0.07-20 mJ) with a delay cable equivalent (50 ns) in the sync channel. Emission decay traces were recorded in 1024 bins over a time span of 50 ns. The instrument response function (IRF) was collected from a light-scattering suspension of silica LUDOX for measurements with dispersed heterostructures and from a ZrO_2 film for measurements with thin-film samples.

Transmission Emission Microscopy (TEM).

Mixed dispersions of NHS-CdSe QDs and either 4-ATP- or TP-CdSe QDs in DMSO were combined. After 24 h, the QDs were deposited onto 300 mesh carbon-coated Cu grids. Samples were placed under vacuum (18 h) to remove DMSO. TEM images were acquired with a JEOL-2010 electron microscope operated at 200 kV.

Appendix S2. Multiexponential decay model to fit time-resolved emission decay traces, using Fluofit software by Picoquant, and representative fits.

Decay traces were fit using a multiexponential reconvolution method according to:

$$I(t) = \int_{-\infty}^{t} IRF(t') \sum_{i=1}^{n} A_i \exp\left(\frac{t-t'}{\tau_i}\right) dt' \quad \text{(S1)}$$

where I(t) is intensity, IRF(t') is the instrument response function, t is time, τ_i is the lifetime of the ith component, and A_i is the amplitude of the ith component.

The intensity-weighted average excited state lifetimes ($\langle\tau\rangle$) were calculated as follows:

$$\langle\tau\rangle = \frac{\sum A_i \tau_i^2}{\sum A_i \tau_i} \quad \text{(S2)}$$

The monoexponential (left), biexponential (middle), and triexponential (right) fitting functions are shown for ZrO_2-CdSe-NHS thin films at 700 nm as a representative example. The top graph in each set represents the time-resolved decay traces (blue), IRF (red), and multiexponential fits from equation s2 (black) with the resulting chi-square values. Bottom graphs represent the corresponding residuals.

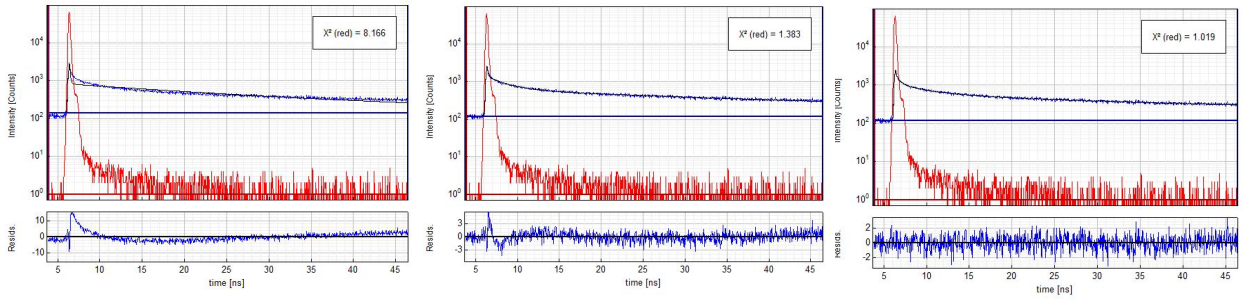

References:

1. Allara, D. L.; Nuzzo, R. G., Spontaneously Organized Molecular Assemblies. 2. Quantitative Infrared Spectroscopic Determination of Equilibrium Structures of Solution-Adsorbed n-Alkanoic Acids on an Oxidized Aluminum Surface. Langmuir 1985, 1 (1), 52-66.

2. Arnold, R.; Azzam, W.; Terfort, A.; Wöll, C., Preparation, Modification, and Crystallinity of Aliphatic and Aromatic Carboxylic Acid Terminated Self-Assembled Monolayers. Langmuir 2002, 18 (10), 3980-3992.

3. Zecchina, A.; Bordiga, S.; Spoto, G.; Marchese, L.; Petrini, G.; Leofanti, G.; Padovan, M., Silicalite Characterization. 2. IR Spectroscopy of the Interaction of Carbon Monoxide with Internal and External Hydroxyl Groups. J. Phys. Chem. 1992, 96 (12), 4991-4997.

4. Frey, B. L.; Corn, R. M., Covalent Attachment and Derivatization of Poly(l-lysine) Monolayers on Gold Surfaces As Characterized by Polarization−Modulation FT-IR Spectroscopy. Anal. Chem. 1996, 68 (18), 3187-3193.

5. Xiao, S.-J.; Brunner, S.; Wieland, M., Reactions of Surface Amines with Heterobifunctional Cross-Linkers Bearing Both Succinimidyl Ester and Maleimide for Grafting Biomolecules. J. Phys. Chem. B 2004, 108 (42), 16508-16517.

6. Deacon, G. B.; Phillips, R. J., Relationships Between the Carbon-Oxygen Stretching Frequencies of Carboxylato Complexes and the Type of Carboxylate Coordination. Coord. Chem. Rev. 1980, 33 (3), 227-250.

7. Dibbell, R. S.; Soja, G. R.; Hoth, R. M.; Watson, D. F., Photocatalytic Patterning of Monolayers for the Site-Selective Deposition of Quantum Dots onto TiO_2 Surfaces. Langmuir 2007, 23 (6), 3432-3439.

8. Charpentier, T. V. J.; Neville, A.; Millner, P.; Hewson, R.; Morina, A., An Investigation of Freezing of Supercooled Water on Anti-Freeze Protein Modified Surfaces. J. Bionic Eng. 2013, 10 (2), 139-147.